

Statistical modelling of propagation and interaction of solitons in fiber-optic lines

VITALIY LUKINOV

Novosibirsk national research state university

Department of applied mathematic

Institute of Computational Mathematics and Mathematical Geophysics SB RAS

Department of statistical modelling in physics

prospect Akademika Lavrentjeva 6, Novosibirsk, 630090

RUSSIA

Vitaliy.Lukinov@gmail.com

Abstract: The paper presents a constructive way to model the soliton propagate described by the classical nonlinear Schrodinger equation. We investigate the performance of the nonlinear inverse synthesis (NIS) method, in which the information is encoded directly onto the continuous part of the nonlinear signal spectrum. We consider the features of statistical calculations requiring large computational resources on BFNT stage of NIS method. We investigate numerically the feasibility of merging the NIS technique in a burst mode with high spectral efficiency methods showing a performance improvement.

Key-Words: Statistical modelling, Monte Carlo methods, SDE, nonlinear Schrodinger equation, solitons, optical fiber

1 Introduction

The rapidly increasing demand on communication speed is exerting great pressure on the networks infrastructure at every scale, which explains the real motivation behind all optical communications research. Since the introduction of fiber-optic communications in the late 1970s, many technological advances, such as erbium-doped fiber amplifiers, wavelength division multiplexing (WDM), dispersion management, forward error correction, and Raman amplification, have been developed to enable the exponential growth of data traffic. However, the continuing bandwidth demand is pushing the required capacity close to the theoretical limit of the standard single-mode fiber (SSFM), which is imposed by the fibers nonlinearity effects (Kerr effect) [1]. In recent years, there have been extensive efforts in attempting to surpass the Kerr nonlinearity limit through various nonlinearity compensation techniques. However, there are still many limitations and challenges in applying the aforementioned nonlinear compensation methods, because the transmission technologies utilized in optical fiber communication systems were originally developed for linear (radio or open space) communication channels. Therefore the true limits of nonlinear fiber channels are yet to be found.

The propagation of optical signals in fiber can be accurately modelled by the nonlinear Schrodinger

equation (NLSE) [1], which describes the continuous interplay between dispersion and nonlinearity. It is well known that the NLSE (without perturbation) belongs to the class of integrable nonlinear systems. In particular, this means that the NLSE allows the existence of a special type of solutions: highly robust nonlinear waves, called solitons. Solitons were proposed as the information carriers for the high-capacity fiber-optic communications. In this article we use multi-processor computing to model the soliton propagate where the number of nuclei runs into hundreds of thousands puts forward Monte Carlo methods (MCM) the most adapted to parallel calculations, both from the point of view of the simplicity of parallelizing the algorithms and the necessity of carrying out a huge number of identical calculations. The highest efficiency of using MCM in parallel calculations is achieved on modeling long term random processes, in particular, the solutions of stochastic differential equations. By modeling on supercomputer independent from each other trajectories of the solutions of SDE, one can evaluate any required functionals from the solutions with an assigned accuracy. The calculations were carried out on the cluster of NCC-30T of Siberian Supercomputer Center at the ICM&MG SB RAS.

2 Nonlinear Schrodinger equation

Let us consider as a model of the propagation of a complex slowvarying optical-field envelope $q(z,t)$ along a single-mode lossless optical fiber the NLSE

$$iq_z - \frac{\beta_2}{2}q_{tt} + \gamma q|q|^2 = 0 \tag{1}$$

where z is the propagation distance and t is the time in the frame co-moving with the group velocity of the envelope. Here, we consider the case of the constant chromatic dispersion coefficient is $\beta_2 < 0$ in Eq. 1 and hence deal with the so-called focusing type of NLSE. The higher-order dispersion terms are not considered here. The instantaneous Kerr nonlinearity coefficient γ is

$$\gamma = n_2\omega_0/cA_{em} \tag{2}$$

where n_2 is the refractive index, A_{em} is an effective mode area, c is the vacuum speed of light and ω_0 is the angular carrier frequency.

For further purposes we will use NLSE in the normalized form:

$$iq_z - q_{tt} + q|q|^2 = 0 \tag{3}$$

which can be obtained through the following rescaling of variables:

$$\frac{t}{T_s} \rightarrow t, \quad \frac{z}{Z_s} \rightarrow z, \quad \sqrt{\gamma Z_s} \rightarrow q \tag{4}$$

where T_s is a free parameter (e.g., a characteristic time scale of the input waveform) and the associated space scale is $Z_s = T_s^2\beta_2$. Note that all the quantities q , t , and z in the normalized equation are now dimensionless.

3 IST method

3.1 Forward Nonlinear Fourier transform

Similarly to the forward FT, the purpose of the FNFT is to decompose the signal into the IST spectral data. This operation is achieved by solving the Zakharov-Shabat problem (ZSP) [3]. The latter corresponds to a scattering problem for a non-Hermitian (in the case of anomalous dispersion) Dirac-type system of equations for two auxiliary functions $v_1(t)$, $v_2(t)$, with the NLSE input pulse profile, $q(0,t) \equiv q(t)$, serving as an effective potential entering into these equations:

$$\frac{dv_1}{dt} = q(t)v_2 - i\zeta v_1, \quad \frac{dv_2}{dt} = -\bar{q}(t)v_1 + i\zeta v_2 \tag{5}$$

Here, ζ is a (generally complex) eigenvalue, $\zeta = \xi + i\eta$, $\bar{q}(t)$ is the complex conjugation of the potential

$q(t)$, which is assumed to decay as $t \rightarrow \pm\infty$ (for the exact conditions imposed on the decay rate, see [3]). In order to define the continuous part of the nonlinear spectrum (for real $\zeta = \xi$) one fixes two linearly-independent Jost solutions of equation (5) as:

$$\Phi(t, \xi) = [\phi_1, \phi_2]^T, \quad \tilde{\Phi}(t, \xi) = [\bar{\phi}_2, -\bar{\phi}_1]^T, \tag{6}$$

with the initial condition at the left end:

$$\Phi(t, \xi)|_{t \rightarrow -\infty} = [e^{-i\xi t}, 0]^T \tag{7}$$

In the same way, we fix two other Jost solutions,

$$\Psi(t, \xi) = [\psi_1, \psi_2]^T, \quad \tilde{\Psi}(t, \xi) = [\bar{\psi}_2, -\bar{\psi}_1]^T, \tag{8}$$

at the right end:

$$\Psi(t, \xi)|_{t \rightarrow +\infty} = [0, e^{i\xi t}]^T \tag{9}$$

These two solution sets are linearly dependent and can be expressed through the Jost scattering coefficients $a(\xi)$ and $b(\xi)$ as:

$$\begin{aligned} \Phi(t, \xi) &= a(\xi)\tilde{\Psi}(t, \xi) + b(\xi)\Psi(t, \xi) \\ \tilde{\Phi}(t, \xi) &= -\bar{a}(\xi)\Psi(t, \xi) + \bar{b}(\xi)\tilde{\Psi}(t, \xi) \end{aligned} \tag{10}$$

The reflection coefficient, giving the continuous part of the nonlinear spectrum, is defined as:

$$r(\xi) = \bar{b}(\xi)/a(\xi) \tag{11}$$

The solitons correspond to the complex eigenvalues ζ_n , where $a(\zeta_n) = 0$. The forward NFT maps the initial field, $q(0,t)$, onto a set of scattering data $\Sigma = [(r(\xi)), \xi \text{ is real}; (\zeta_n, \gamma_n = (b(\zeta_n)a'_\zeta(\zeta_n))^{-1})]$, where the index n runs over all discrete eigenvalues of the ZSP (discrete non-dispersive part of the nonlinear spectrum). Herein, the complex-valued function $r(\xi)$ of the real argument ξ (nonlinear spectrum) is similar to the usual Fourier spectrum. Therefore, within the NIS method we use this continuous part of the nonlinear spectrum, $r(\xi)$, to encode and transmit the information, and ξ plays the role of the frequency. The nonlinear spectral (NS) function, defined as:

$$N(\omega) = -r(\xi)|_{\xi=-\omega/2} \tag{12}$$

serves as the direct nonlinear analog of the Fourier spectrum, tending to the ordinary FT of $q(0,t)$ in the linear limit.

3.2 Backward Nonlinear Fourier transform

The Backward Nonlinear Fourier transform (BNFT) is an inverse operation for the forward NFT that maps

the scattering data \sum onto the field $q(t)$ (or, more generally, onto $q(t, z)$) in the time domain. This can be achieved via solving the Gelfand-Levitan-Marchenko equation (GLME) for the unknown function $K(t, x)$ [4, 5, 6, 7]. In the NIS method described above, we consider only the soliton-free case, for which the GLME can be written as:

$$K(t, x) + F(t + x) + \int_{-\infty}^t ds \int_{-\infty}^t dr K(t, r) \bar{F}(s + y) F(r + s) = 0 \tag{13}$$

Here the kernel $F(x)$ is the linear FT of $r(\xi)$ given in terms of spectrum

$$F(x) = \frac{1}{2\pi} \int_{-\infty}^{+\infty} r(\xi) e^{-i\xi x} d\xi \tag{14}$$

Solving equation (24) for $K(t, x)$, the inverse NFT of $r(\xi)$ can be obtained as:

$$q(t) = 2 \lim_{x \rightarrow t-0} K(t, x) \tag{15}$$

4 Numerical methods

4.1 Computing the continuous spectrum

The continuous spectrum (i.e., Jost coefficients $a(\xi)$ and $b(\xi)$ and the reflection coefficient $r(\xi)$), can be computed by directly integrating the Zakharov-Shabat system (5) and then evaluating the limits for the corresponding Jost function components as:

$$\begin{aligned} a(\xi) &= \lim_{t \rightarrow +\infty} \phi_1(t, \xi) e^{i\xi t} \\ b(\xi) &= \lim_{t \rightarrow +\infty} \phi_2(t, \xi) e^{-i\xi t} \end{aligned} \tag{16}$$

PCA method can be used to solve the ZSP (5). It can be implemented effectively in parallel to reduce the computational time [8, 9]. Although the ZSP is defined on the infinite time line, we must truncate the potential outside a sufficiently large interval in order to make the numerical solution possible. As a result, we reduce the infinite-line spectral problem to a problem with a finite-width potential and to the corresponding boundary conditions for the truncated potential.

The potential $q(t)$ is truncated outside a range $(T_0; T_0)$. Inside this range, $q(t)$ is chosen to be constant, $q_n = q(t_n)$, on each elementary subinterval (or numerical time-step) $(t_n - \Delta t/2; t_n + \Delta t/2)$, where $t_n = -T_0 + n\Delta t$, $\Delta t = T_0/M$ is the time step, and $2M + 1$ is the total number of mesh nodes inside the considered range. The idea of the PCA method is based on the fact that equation (5) can be solved

exactly inside each elementary mesh interval for an arbitrary value of the spectral parameter ξ as:

$$\Phi(t_n + \Delta t/2, \xi) = T(q_n, \xi) \Phi(t_n - \Delta t/2, \xi), \tag{17}$$

where transition matrix $T(q_n, \xi)$ is given by

$$T(q_n, \xi) = \exp \left[\Delta t \begin{pmatrix} -i\xi & q_n \\ -\bar{q}_n & i\xi \end{pmatrix} \right] \tag{18}$$

The scattering problem can be solved by propagating the solution iteratively, starting from $-T_0$ to the right boundary T_0 , using the set of transfer matrices $T(q_n, \xi)$ given by equation (4.1). The final result can be expressed as:

$$\begin{aligned} \Phi(T_0 - \Delta t/2, \xi) &= \prod(\xi) \Phi(-T_0 + \Delta t/2, \xi) \\ \prod(\xi) &= \prod_{n=1}^{2M} T(q_n, \xi) \end{aligned} \tag{19}$$

The initial condition defined at the right truncation end can be written as:

$$\Phi(-T_0 - \Delta t/2, \xi) = (1, 0)^T e^{-i\xi(-T_0 - \Delta t/2)} \tag{20}$$

Then, at the left end of the full interval we have:

$$\Phi(T_0 - \Delta t/2, \xi) = \frac{a(\xi) e^{-i\xi(T_0 - \Delta t/2)}}{b(\xi) e^{i\xi(T_0 - \Delta t/2)}} \tag{21}$$

and, therefore, the Jost coefficients are given by:

$$\begin{aligned} a(\xi) &= \prod_{11}(\xi) e^{2i\xi T_0} \\ b(\xi) &= \prod_{21}(\xi) e^{-i\xi \Delta t}, \end{aligned} \tag{22}$$

where $\prod_{11}(\xi)$ and $\prod_{21}(\xi)$ are corresponding components of matrix $\prod(\xi)$. In general, when the potential $q(t)$ is truncated outside the interval (T_{min}, T_{max}) with arbitrary borders, the expression (22) can be modified as:

$$\begin{aligned} a(\xi) &= \prod_{11}(\xi) e^{i\xi(T_{max} - T_{min})} \\ b(\xi) &= \prod_{21}(\xi) e^{-2i\xi(T_{max} + T_{min} - \Delta t)}, \end{aligned} \tag{23}$$

From (19), one can see that the transfer matrixes $T(q_n, \xi)$ can be calculated independently of each other. As a result, the PCA algorithm can be easily implemented in parallel to reduce the computational time for high-speed NIS-based systems.

4.2 Computing the BNFT

The GLME can be rewritten in the form of two coupled integrals, which are more convenient for numerical calculations:

$$\begin{aligned}
 A_1(x, t) + \int_{-\infty}^x F(t+x)\bar{A}_2(x, y)dy &= 0 \\
 A_2(x, t) - \int_{-\infty}^x F(t+x)\bar{A}_1(x, y)dy &= F(x+t), x > t
 \end{aligned}
 \tag{24}$$

where $F(t)$ is the linear backward FT of $r(\xi)$. For the numerical analysis we use the following change of the variables [43]:

$$u(x, s) = \bar{A}_1(x, x-s), \quad v(x, \tau) = \bar{A}_2(x, \tau-x),
 \tag{25}$$

so the GLME (24) can be rewritten in the form:

$$\begin{aligned}
 u(x, s) + \int_{\frac{s}{\tau}}^{2x} F(t-s)v(x, \tau)d\tau &= 0 \\
 v(x, \tau) - \int_0^{\frac{s}{\tau}} F(t-s)u(x, s)ds &= F(\tau)
 \end{aligned}
 \tag{26}$$

Functions $u(x, s)$ and $v(x, s)$ are defined inside the interval $0 \leq \tau \leq 2x \leq 2T_0$. The BNFT mapping $r(\xi)$ onto the time domain is then given by

$$q(x) = 2v(x, 2x-0)
 \tag{27}$$

Following the discretization procedure provided in [9], we divide the interval $\tau \leq 2T_0$, where the function $F()$ is known, into segments of length $h = 2T_0/N$. The discrete variables n, s_k , and x_m are defined as:

$$\begin{aligned}
 s_k &= h(k-1)/2, \quad k = 1, 2, \dots, m \\
 \tau_n &= h(n-1)/2, \quad n = 1, 2, \dots, m \\
 x_m &= mh/2, \quad m = 1, 2, \dots, N
 \end{aligned}
 \tag{28}$$

We also define the grid functions:

$$u_n^{(m)} = u(x_n, \tau_m), \quad v_n^{(m)} = v(x_n, \tau_m), \quad F_n = F(nh)
 \tag{29}$$

Using the rectangular quadrature scheme to approximate the integrals in equation (26), one obtains the following discrete form of the GLME:

$$\begin{aligned}
 u_k^{(m)} + h \sum_{n=k}^m \bar{F}_{n-k} v_n^{(m)} &= 0 \\
 v_n^{(m)} - h \sum_{k=1}^m F_{n-k} u_k^{(m)} &= F_n
 \end{aligned}
 \tag{30}$$

The m th mesh element of the BNFT (in the time domain) is then given by:

$$q^{(m)} = v_m^{(m)}
 \tag{31}$$

Equations (30) can now be written in a matrix form as:

$$\mathbf{G}^m = \begin{pmatrix} u^{(m)} \\ v^{(m)} \end{pmatrix} = \mathbf{b}^{(m)}
 \tag{32}$$

where $\mathbf{b}^{(m)}$ is formed from the zero vector of dimension m and the vector of dimension m with components F_n ; \mathbf{G}^m in (32) is a square matrix of dimensions $2m \times 2m$, which has the following form:

$$\mathbf{G}^m = \begin{pmatrix} \mathbf{E}^{(m)} & h\bar{\mathbf{F}}^{(m)} \\ -h\mathbf{F}^{(m)} & \mathbf{E}^{(m)} \end{pmatrix}
 \tag{33}$$

Here, $\mathbf{E}^{(m)}$ is the identity (unity) $m \times m$ matrix, $\mathbf{F}^{(m)}$ is the lower triangular Toeplitz $m \times m$ matrix of the form:

$$\mathbf{F}^m = \begin{pmatrix} F_0 & 0 & \dots & 0 \\ F_1 & F_0 & \dots & 0 \\ \vdots & \vdots & \vdots & \vdots \\ F_m & F_{m-1} & \dots & F_0 \end{pmatrix}
 \tag{34}$$

and $\bar{\mathbf{F}}^{(m)}$ is the Hermitian conjugate of the matrix $\mathbf{F}^{(m)}$. For constructing statistical algorithms we can rewrite equation (32) in form

$$\begin{pmatrix} u^{(m)} \\ v^{(m)} \end{pmatrix} = \mathbf{G}_0^m \begin{pmatrix} u^{(m)} \\ v^{(m)} \end{pmatrix} + \mathbf{b}^{(m)},
 \tag{35}$$

where substochastic matrix \mathbf{G}_0^m is derived from \mathbf{G}^m as

$$\mathbf{G}_0^m = \begin{pmatrix} 0 & -h\bar{\mathbf{F}}^{(m)} \\ h\mathbf{F}^{(m)} & 0 \end{pmatrix}
 \tag{36}$$

One of the approaches to constructing statistical algorithms for solving (36) is based on the following presentation

$$u = (I - K_c)^{-1}h = h + R_c h, \quad R_c = \sum_{i=1}^{\infty} K_c^i
 \tag{37}$$

5 Certain Nonlinear Schrodinger equation

5.1 Problem

The aim of this work is to study the nonlinear effects in the propagation of laser pulses in a long optical fiber, arising due to the modulation instability. The propagation of long pulse in an optical fiber is described by the linear Schrodinger equation [1]:

$$\frac{\partial A}{\partial z} + \frac{1}{c} \frac{\partial A}{\partial t} = i \frac{|\beta_2|}{2} \frac{\partial^2}{\partial t^2} A + i\gamma |A|^2 A - \alpha A,
 \tag{38}$$

where $A(t, z)$ is the amplitude of the electromagnetic field on the carrier frequency $\omega_0 = 2\pi n_0/\lambda_0$, the amplitude is normalized by power $P = |A|^2$; c is the speed of light in an optical fiber with a refractive index n_0 ; $\beta_2 = -10 \text{ km}^{-1} \cdot \text{nm}^{-2}$ is dispersion on wavelength 1550 nm; $\gamma = 3 \text{ W}^{-1} \cdot \text{km}^{-1}$ is the nonlinearity coefficient; $\alpha = 0.17 \text{ dB/km}$ is the coefficient of optical losses.

The boundary condition at the input to the optical fiber is given as the sum of Gaussian pulse with a width at half maximum $T_0 = 100 \text{ ns}$ and noise amplitude $A_n(t)$:

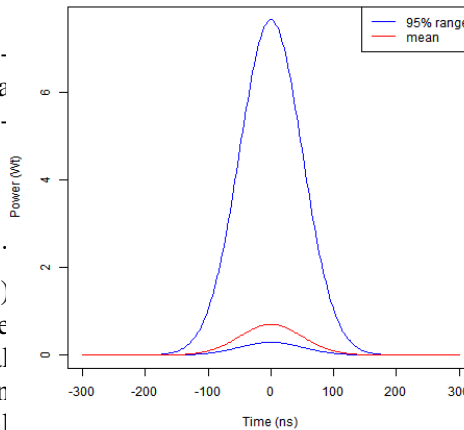
$$A(t, 0) = \sqrt{P_0} \exp\left(-\frac{t^2}{T_0^2} 2 \ln 2\right) \sqrt{\frac{4 \ln 2}{\pi}} + A_n(t). \tag{39}$$

Here $P_0 = \varepsilon_0/T_0$ is the average power of the pulse of energy ε_0 . Random noise has a nonzero spectral density power $P_n(\omega) = |A_n(\omega)|^2$ ($P_n(\omega) = \varepsilon_n/\Delta$) in the spectral range of $\Delta = 1 \text{ nm}$ relative to the central carrier frequency ω_0 ; ε_n is the average noise energy over the period $\tau = 2 \text{ ms}$ pulse. The ratio of pulse energy and noise $\varepsilon_0/\varepsilon_n$ is taken equal to 0.7 [2]

5.2 Numerical calculations

For the numerical solution of equation (38) was used the above described modified NIS scheme with In calculations time $T = 1 \text{ ms}$ was considered with the number of time points $N = 2^{20}$. Step by spatial variable was $\Delta z = 0.1 \text{ mm}$. As the initial distribution was set to Gaussian pulse with duration at half maximum intensity of 100ns and variable peak power P_p , namely $A(0, t) = \sqrt{P_p} \exp(-t^2/2T_0^2)$, and white Gaussian noise with spectral band 1nm was added to it. Number of modelled impulses was 10^6 .

Impulse range transmitted over 6 km



6 Conclusion

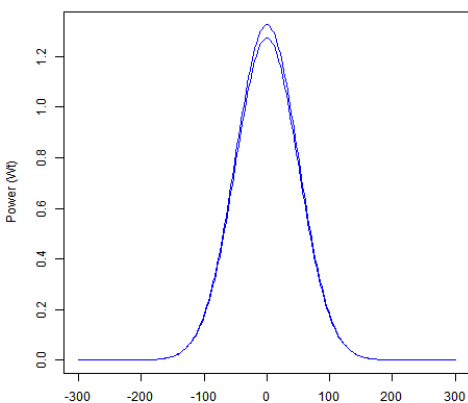
The results in the previous sections demonstrate theoretical and the corresponding NIS numerical methods. Numerical calculation confirmed that for the NIS method a performance improvement can be achieved by using parallel statistical methods on BNFT stage.

Acknowledgements: The reported study was funded by RFBR according to the research project No 17-01-00698-a. It was also partially supported by Novosibirsk national research state university.

References:

- [1] G. Agrawal, Nonlinear fiber optics, *Academic Press*, New York , 1996
- [2] S.T. Lee, J.E. Prilepsy, S.,K. Turitsyn, Non-linear inverse synthesis for high spectral efficiency transmission in optical fibers. *OPTICS EXPRESS, Vol. 22, No 22* , 2014.
- [3] V. E. Zakharov and A. B. Shabat, Exact theory of two-dimensional self-focusing and one-dimensional selfmodulation of waves in nonlinear media, *Sov. Phys. JETP 34, 6269* , 1972.
- [4] M. J. Ablowitz, D. J. Kaup, A. C. Newell, and H. Segur, The inverse scattering transform-Fourier analysis for nonlinear problems, *Stud. Appl. Math. 53, 249315*, 1974.
- [5] V. E. Zakharov, S. V. Manakov, S. P. Novikov, and L. P. Pitaevskii, Theory of Solitons. The Inverse Scattering Method. *Consultants Bureau, New York* , 1984.

Initial impulse range



- [6] M. J. Ablowitz and H. Segur, Solitons and the Inverse Scattering Transform. *SIAM, Philadelphia*, 1981.
- [7] A. C. Newell, Solitons in mathematics and physics. *SIAM, Philadelphia*, 1985.
- [8] G. Boffetta and A. R. Osborne, Computation of the direct scattering transform for the nonlinear Schroedinger equation, *J. Comput. Phys.* 102(2), 252264, 1992.
- [9] O. V. Belai, L. L. Frumin, E. V. Podivilov, and D. A. Shapiro, Efficient numerical method of the fiber Bragg grating synthesis, *J. Opt. Soc. Am. B* 24(7), 14511457, 2007.
- [10] T.A. Averina and S.S Artemiev, Analysis of Accuracy of Monte Carlo Methods in Solving Boundary Value Problems by Probabilistic Representations, *Sib. Zh. Vych. Mat.*, (2008) , vol. 11, no. 3, pp. 239-250.